

Geomorphometry and spatial hydrologic modelling

1 *Peckham, S.D.*

2 **how can DEMs be used for spatial**
 3 **hydrologic modelling? • what methods**
 4 **are commonly used to model hydrologic**
 5 **processes in a watershed? • what kinds**
 6 **of preprocessing tools are typically**
 7 **required? • what are some of the key**
 8 **issues in spatial hydrologic modelling?**

9 25.1 Introduction

10 **Spatial hydrologic modelling** is one of the
 11 most important applications of the geomorpho-
 12 metric concepts discussed in this book. The sim-
 13 ple fact that flow paths follow the topographic
 14 gradient results in an intimate connection be-
 15 tween geomorphometry and hydrology, and this
 16 connection has driven much of the progress in
 17 the field of geomorphometry. It also continues
 18 to help drive the development of new technolo-
 19 gies for creating high-quality and high-resolution
 20 DEMs, such as LiDAR. Like most other types of
 21 physically-based models, hydrologic models are
 22 built upon the fundamental principle that the
 23 mass and momentum of water must be conserved
 24 as it moves from place to place, whether it is on
 25 the land surface, below the surface or evaporat-
 26 ing into the atmosphere. While this sounds like
 27 a simple enough idea, it provides a powerful con-
 28 straint that makes predictive modelling possible.
 29 When mass and momentum conservation is sim-
 30 ilarly applied to sediment, it is possible to create
 31 **landscape evolution models** that predict the

spatial erosion and deposition of sediment and
 32 contaminants. 33

While hydrologic models have been around
 34 for several decades, it is only in the last fifteen
 35 years or so that computers have become powerful
 36 enough for fully spatial hydrologic models to be
 37 of practical use. **Spatially-distributed** hydro-
 38 logic models treat every grid cell in a DEM as a
 39 control volume which must conserve both mass
 40 and momentum as water is transported to, from,
 41 over and below the land surface. The control vol-
 42 ume concept itself is quite simple: what flows in
 43 must either flow out through another face or ac-
 44 cumulate or be consumed in the interior. Con-
 45 versely, the amount that flows out during any
 46 given time step cannot exceed the amount that
 47 flows in during that time step plus the amount al-
 48 ready stored inside. However, the number of grid
 49 cells required to adequately resolve the transport
 50 within a river basin, in addition to the small size
 51 of the timesteps required for a spatial model to
 52 be numerically stable, results in a computational
 53 cost that until recently was prohibitive. 54

Remark 118: *Since flow paths follow the topographic gradient, there is an intimate connection between geomorphometry and hydrology. Spatial hydrologic models make use of several DEM-derived grids especially grids of slope, aspect (flow direction) and contributing area.*

For a variety of reasons, including the com-
 55 putational cost of fully spatial models and the 56
 57
 58

1 fact that data required for more advanced mod- 48
 2 els is often unavailable, researchers have invested 49
 3 a great deal of effort into finding ways to sim- 50
 4 plify the problem. This has resulted in many 51
 5 different types of hydrologic models. For ex- 52
 6 ample, **lumped models** employ a small num- 53
 7 ber of “*representative units*” (very large, but 54
 8 carefully-chosen control volumes), with simple 55
 9 methods to route flow between the units. An- 56
 10 other strategy for reducing the complexity of hy- 57
 11 drologic models is to use concepts such as **hy-** 58
 12 **drologic similarity** to essentially collapse the
 13 2D (or 3D) problem to a 1D problem. For ex-
 14 ample, TOPMODEL (Beven and Kirkby, 1979)
 15 defines a **topographic index** or wetness in-
 16 dex and then lumps all grid cells with the same
 17 value of this index together under the assump-
 18 tion that they will have the same hydrologic re-
 19 sponse. Similarly, many models lump together
 20 all grid cells with the same elevation (via the
 21 **hypsothetic curve** or **area-altitude func-**
 22 **tion**) to simplify the problem of computing cer-
 23 tain quantities such as snowmelt. All grid cells
 24 with a given **flow distance** to a basin outlet can
 25 also be lumped together (via the **width func-**
 26 **tion** or **area-distance function**) and this is the
 27 main idea behind the concept of the **instanta-**
 28 **neous unit hydrograph**. While models such
 29 as these can be quite useful and require less in-
 30 put data, they all employ simplifying assump-
 31 tions that prevent them from addressing general
 32 problems of interest. In addition, these assump-
 33 tions are often difficult to check and are therefore
 34 a source of uncertainty. In essence, these types
 35 of models gain their speed by mapping many dif-
 36 ferent (albeit similar) 3D flow problems to the
 37 same 1D problem in the hope that the lost differ-
 38 ences don’t matter much. While geomorphome-
 39 tric grids are used to prepare input data for vir-
 40 tually all hydrologic models, fully spatial models
 41 make direct use of these grids. For this reason,
 42 and in order to limit the scope of the discussion,
 43 this chapter will focus on fully-spatial models.

44 There are now many different spatial hydro-
 45 logic models available, and their popularity, so-
 46 phistication and ease-of-use continues to grow
 47 with every passing year. A few representa-

tive examples of some highly-developed spa- 48
 tial models are: **Mike SHE** (a product of 49
 Danish Hydraulics Institute, Denmark), Grid- 50
 ded Surface Subsurface Hydrologic Analysis 51
 (**GSSHA**), **CASC2D** (Julien et al., 1995; Og- 52
 den and Julien, 2002), **PRMS** (Leavesley et al., 53
 1991), **DHVSM** (Wigmosta et al., 1994) and 54
TopoFlow. Rather than attempt to review or 55
 compare various models, the main goal of this 56
 chapter is to discuss basic concepts that are com- 57
 mon to virtually all spatial hydrologic models. 58

Remark 119: *Hydrologic processes in a watershed (e.g. snowmelt) may be modelled with either simple methods (e.g. degree-day) or very sophisticated methods (e.g. energy-balance), based partly on the input data that is available.*

59
 60
 61 It will be seen throughout this chapter that
 62 grids of elevation, slope, aspect and contribut-
 63 ing area all play fundamental roles in spatial hy-
 64 drologic modelling. Some of these actually play
 65 multiple roles. For example, slope and aspect are
 66 needed to determine the velocity of surface (and
 67 subsurface) flow, but also determine the amount
 68 of solar radiation that is available for evapotran-
 69 spiration and melting snow. The DEM grid spac-
 70 ing that is required depends on the application,
 71 but as a general rule should be sufficient to ad-
 72 equately resolve the local hillslope scale. This
 73 scale marks the transition in process dominance
 74 from hillslope processes to channel processes. It
 75 is typically between 10 and 100 m, but may be
 76 larger for arid regions. As a result of the Shut-
 77 tle Radar Topography Mission (SRTM), DEMs
 78 with a grid spacing less than 100 m are now avail-
 79 able for much of the Earth. In addition, LiDAR
 80 DEMs with a grid spacing less than 10 m can
 81 now be purchased from private firms for specific
 82 areas. Many of the DEMs produced by govern-
 83 ment agencies (e.g. the U.S. Geological Survey
 84 and Geoscience Australia) now use an algorithm
 85 such as ANUDEM (Hutchinson, 1989) to produce
 86 “*hydrologically sound*” DEMs which makes them

1 better suited to hydrologic applications (see also
2 §2.3.2).

3 This chapter has been organised as follows.
4 §25.2 discusses several key hydrologic processes
5 and how they are typically incorporated into spa-
6 tial models. Note that spatial hydrologic models
7 integrate many branches of hydrology and there
8 are many different approaches for modelling any
9 given process, from simple to very complex. It
10 is therefore impossible to give a complete treat-
11 ment of this subject in this chapter. For a greater
12 level of detail the reader is referred to textbooks
13 and monographs such as (Henderson, 1966; Ea-
14 gleson, 1970; Freeze and Cherry, 1979; Welty
15 et al., 1984; Beven, 2000; Dingman, 2002; Smith,
16 2002). The goal here is to highlight the most
17 fundamental concepts that are common between
18 spatial models and to show how they incorporate
19 geomorphometric grids. §25.3 discusses scale is-
20 sues in spatial hydrologic modelling. §25.4 pro-
21 vides a brief discussion of preprocessing tools
22 that are typically needed in order to prepare re-
23 quired input data. §25.5 is a simple case study in
24 which a model called TopoFlow is used to simu-
25 late the hydrologic response of a small ungauged
26 watershed in the Baranja Hill case study.

27 25.2 Spatial hydrologic modelling: 28 processes and methods

29 25.2.1 The control volume concept

30 Spatially-distributed hydrologic models are
31 based on applying the control volume concept
32 to every grid cell in a digital elevation model
33 (DEM). It is helpful to imagine a box-shaped
34 control volume resting on the land-surface such
35 that its top and bottom faces have the x and y
36 dimensions of a DEM grid cell and such that the
37 height of the box is greater than the local wa-
38 ter depth (see Fig. 25.1). Water flowing from
39 cell to cell across the land-surface flows hori-
40 zontally through the four vertical faces of this
41 box, according to the D8, D-Infinity or Mass
42 Flux method (see §7.3.2). For overland flow,
43 the entire bottom of the box may be wetted and
44 2D modelling of the flow is possible. For chan-

nelised flow, the grid cell dimensions are typically
45 much larger than the channel width, so channel
46 width must be specified as a separate grid, along
47 with an appropriate sinuosity in order to prop-
48 erly compute mass and momentum balance. 49

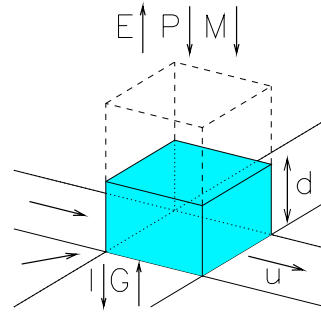


Fig. 25.1: A grid-cell control volume resting on the
land-surface and filled with water to a depth, d . Pre-
cipitation, P , snowmelt, M , evapotranspiration, E ,
infiltration, I , and groundwater seepage, G add or
remove water from the top and bottom faces, while
surface water flows through the four vertical faces.
Overland flow is shown, but a grid cell may instead
contain a single, sinuous channel with a width less
than the grid spacing.

Runoff-generating processes can be thought of
50 as “injecting” flow vertically through the top
51 face of the box, as in the case of rainfall and
52 snowmelt, or through the bottom of the box, as
53 in the case of seepage from the subsurface as a re-
54 sult of the local water table rising to the surface.
55 Similarly, infiltration and evapotranspiration are
56 vertical flux processes that result in a loss of wa-
57 ter through either the bottom or top faces of the
58 box, respectively. If a grid cell contains a chan-
59 nel, then the volume of surface water stored in
60 the box depends on the channel dimensions and
61 water depth, d , otherwise it depends on the grid
62 cell dimensions and water depth. 63

The net vertical flux into the box may be re-
ferred to as the **effective rainrate**, R , and is
64 the runoff that was generated within the box. It
65 is given by the equation: 66
67

$$R = (P + M + G) - (E + I) \quad (25.2.1)$$

where P is the precipitation rate, M is snowmelt rate, G is the rate of subsurface seepage, E is the evapotranspiration rate and I is the infiltration rate.

Each of these six quantities varies both spatially and in time and is therefore stored as a grid of values that change over time. Each also has units of [mm/hr]. Methods for computing these quantities are outlined in the next few subsections of this chapter. Note that the total runoff from the box is not equivalent to the effective rainrate because it consists of the effective rainrate *plus* any amount that flowed horizontally into the box and was not consumed by infiltration or evapotranspiration. Note also that in order to model the details of subsurface flow, it is necessary to work with an additional “*stack*” of boxes that extend down into the subsurface; e.g. there may be one such box for each of several soil layers.

In many models of fluid flow, fluxes through control volume boundaries (e.g. the vertical faces of the box) are not computed directly. Instead, the boundary integrals are converted to integrals over the interior of the box using the well-known *divergence theorem* (Welty et al., 1984). This results in differential vs. integral equations and requires computing first and second-order spatial derivatives between neighboring cells, typically via finite-difference methods. However, if we assume that flow directions are determined by topography, which is a relatively static quantity, then flow directions between grid cells are fixed and known at the start of a model run. Under these circumstances it is straight-forward and efficient to compute boundary integrals.

25.2.2 The precipitation process

The precipitation process differs from most of the other hydrologic processes at work in a basin in that the precipitation rate must be specified either from measurements (e.g. radar or rain gauges) or as the result of numerical simulation.

All of the other processes are concerned with methods for tracking water that is already in the system as it moves from place to place (e.g. cell to cell or between surface and subsurface). For a small catchment, it may be appropriate to use measured rainrates from a single gauge for all grid cells. For larger catchments and greater realism, however, it is better to use space-time rainfall, which is stored as a grid stack, indexed by time. This grid stack may be created by spatially interpolating data from many different rain gauges. Input data for air temperature (T) is used to determine whether precipitation falls as rain or as snow.

In order to model how temperature decreases with increasing elevation, a grid of elevations can be used together with a lapse rate. If precipitation falls as snow ($T < 0$ °C), then it can be stored as a grid of snow depths that can change in time. If the snowmelt process is modelled, then snowmelt can contribute runoff to any grid cell that has a nonzero snow depth and an air temperature greater than 0 °C.

25.2.3 The snowmelt process

In general, the conversion of snow to liquid water is a complex process that involves a detailed exchange of energy in its various forms between the atmosphere and the snowpack. While air temperature is obviously of key importance, numerous other variables affect the melt rate, including the slope and aspect of the topography, wind speed and direction, the heights of roughness elements (e.g. vegetation) and the snow density to name a few. The **Energy Balance Method** (Marks and Dozier, 1992; Liston, 1995; Zhang et al., 2000) in its various implementations is therefore the most sophisticated method for melting snow, but it is very data intensive. This method consists of numerous equations (see references) and generally makes use of a clear-sky radiation model (see §8.3.1; Dozier (1980) or Dingman (2002, Appendix E)), for modelling the shortwave solar radiation and the **Stephan-Boltzmann law** for modelling the longwave radiation. Most clear-sky radiation models incor-

1 porate topographic effects via slope and aspect
 2 grids extracted from DEMs.

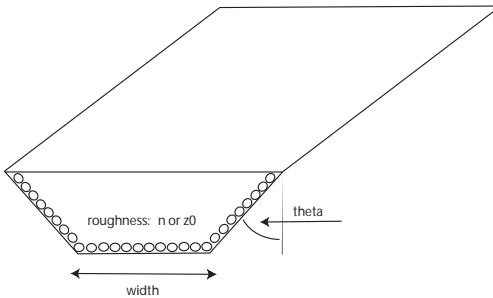


Fig. 25.2: A channel with a trapezoidal cross-section and roughness elements that would connect the centers of two DEM grid cells. The cross-section becomes triangular when the bed width is zero and rectangular when the bank angle is zero.

3 Since the input data required for energy
 4 balance calculations is only available in well-
 5 instrumented watersheds, much simpler meth-
 6 ods for estimating the rate of snowmelt have
 7 been developed such as various forms of the well-
 8 known **Degree-Day Method** (Beven, 2000,
 9 p.80). The basic method predicts the meltrate
 10 using the simple formula:

$$M = c_0 \cdot \Delta T \quad (25.2.2)$$

11 where ΔT is the temperature difference between
 12 the air and the snow and c_0 is an empirical co-
 13 efficient with units of [mm/hr/°C]. In both the
 14 Degree-Day and Energy-Balance methods it is
 15 possible for any input variable to vary spatially
 16 and in time, and many authors suggest that c_0
 17 should vary throughout the melt season. An
 18 example comparison of these two methods is
 19 given by Bathurst and Cooley (1996). What-
 20 ever method is used, the end result is a grid se-
 21 quence of snowmelt rates, M , that is then used
 22 in Eq.(25.2.1).

23 25.2.4 The channel flow process

24 Spatial hydrologic models are based on conserva-
 25 tion of mass and momentum, and many of them
 26 make direct use of D8 flow direction grids and

slope grids to compute the amount of mass and
 momentum that flows into and out of each grid
 cell. The grid cell size is generally chosen to be
 smaller than the hillslope scale and larger than
 the width of the largest channel (see §25.3). Ev-
 ery grid cell then has one channel associated with
 it that extends from the centre of the grid cell to
 the centre of the grid cell that it flows to accord-
 ing to the D8 method. Channelised flow is then
 modelled as an essentially 1D process (in a tree-
 like network of channels), while recognising that
 it will be necessary to store additional channel
 properties for every grid cell such as:

- sinuosity or channel length; 40
- channel bed width; 41
- bank angle (if trapezoidal cross sections are
used) and; 42 43
- a channel roughness parameter. 44

One method for creating these channel property
 grids is discussed in §25.4.

The **kinematic wave** method is the simplest
 method for modelling flow in open channels and
 is available as an option in virtually all spatial
 hydrologic models. This method combines mass
 conservation with the simplest possible treat-
 ment of momentum conservation, namely that
 all terms in the general momentum equation
 (pressure gradient, local acceleration and convec-
 tive acceleration) are negligible except the friction
 and gravity terms. In this case the water surface
 slope, energy slope and bed slope are all equal.
 In addition, the balance of gravity against fric-
 tion (as a shear stress near the bed) results in an
 equation for depth-averaged flow velocity, u ,
 in terms of the flow depth, d , bed slope (rise over
 run), S , and a roughness parameter. If the shear
 stress near the bed is computed using our best
 theoretical understanding of turbulent boundary
 layers (Schlichting, 1960), then this balance re-
 sults in the **law of the wall**:

$$u = (g \cdot R_h \cdot S)^{1/2} \cdot \ln \left(a \cdot \frac{d}{z_0} \right) \cdot \kappa^{-1} \quad (25.2.3)$$

1 Here, g is the gravitational constant, R_h is
 2 the **hydraulic radius**, given as the ratio of the
 3 wetted cross-sectional area and wetted perime-
 4 ter (units of length), a is an integration constant
 5 (given by 0.368 or 0.476, depending on the for-
 6 mulation), z_0 is the **roughness height** (units
 7 of length), and $\kappa \approx 0.408$ is von Karman’s con-
 8 stant.

9 Note that the law of the wall is general and is
 10 also used by the snowmelt energy-balance mod-
 11 els for modelling air flow in the atmospheric
 12 boundary layer. However, in the setting of open-
 13 channel flow, an alternative known as **Man-
 14 ning’s formula** is more often used. Man-
 15 ning’s formula, which was determined by fitting
 16 a power-law to data gives the depth-averaged ve-
 17 locity as:

$$u = \frac{R_h^{2/3} \cdot S^{1/2}}{n} \tag{25.2.4}$$

18 where n is an empirical roughness parameter
 19 with the units of [s/m^{1/3}] required to make the
 20 equation dimensionally consistent. Manning’s
 21 formula agrees very well with the law of the wall
 22 as long as the relative roughness, z_0/d is between
 23 about 10⁻² and 10⁻⁴. This is the range that
 24 is encountered in most open-channel flow prob-
 25 lems. Smaller relative roughnesses are typically
 26 encountered in the case where wind blows over
 27 terrain and vegetation. ASCE Task Force on
 28 Friction Factors (1963) provides a good review
 29 of the long and interesting history that led to
 30 equations Eq.(25.2.3) and Eq.(25.2.4).

31 While the kinematic wave method is an ap-
 32 proximation, it often yields good results, espe-
 33 cially when slopes are steep. The **diffusive
 34 wave** method provides a somewhat better ap-
 35 proximation by retaining one additional term in
 36 the momentum equation, namely the pressure-
 37 gradient (water depth derivative) term. In this
 38 method, the slope of the free water surface is
 39 used instead of the bed slope, and pressure-
 40 related (e.g. backwater) effects can be modelled.
 41 Note that a general treatment of momentum con-
 42 servation uses the full **St. Venant equation**,
 43 which includes the effects of gravity, friction and
 44 pressure-gradients as well as terms for local and

convective acceleration. The convective accel- 45
 eration term corresponds to the net flux of momen- 46
 tum into a given control volume. The most ac- 47
 curate but most computationally demanding ap- 48
 proach retains all of the terms in the St. Venant 49
 equation and is known as the **dynamic wave** 50
 method. Interestingly, the latter two methods 51
 create a water-depth gradient and can thereby 52
 move water across flat areas (e.g. lakes) in a 53
 DEM. These areas have a bed slope of zero and 54
 therefore receive a velocity of zero in the kine- 55
 matic wave method unless they are handled sep- 56
 arately in some manner. Whether the kinematic, 57
 diffusive or dynamic wave method is used, it is 58
 necessary to compute a grid of bed slopes. Given 59
 a DEM with sufficient vertical resolution, the 60
 bed slope can be computed between each grid 61
 cell and its downstream neighbour, as indicated 62
 by a D8 flow grid (see §7). 63

The D8 flow direction grid indicates the 64
 (static) connectivity of the grid cells in a DEM 65
 and can therefore be used directly to simplify 66
 mass and momentum balance calculations. A 67
 D8 flow grid allows fluxes across grid cell bound- 68
 aries to be computed, which makes it possible 69
 to use integral equations instead of differential 70
 equations (Welyt et al., 1984). In particular, the 71
 use of integral equations is simpler because con- 72
 vective acceleration (momentum flux) between 73
 cells can be modelled without computing spatial 74
 derivatives. Grids for the initial flow depth, d , 75
 and velocity, u , are specified, either as all zeros 76
 or computed from channel properties and a base- 77
 level recharge rate. Given the cross-sectional 78
 shape (e.g. trapezoidal) and length, L , of each 79
 channel, the volume of water in the channel 80
 can be computed as $V = A_c \cdot L$, where A_c is 81
 the cross-sectional area. An outgoing discharge, 82
 $Q = u \cdot A_c$, can also be computed for every grid 83
 cell. For each time step, the change in volume 84
 $\Delta V(i, t)$ for pixel i can then be computed as: 85

$$= \Delta t \cdot \left[R(i, t) \cdot \Delta x \cdot \Delta y - Q(i, t) + \sum_{k \in N} Q(k, t) \right] \tag{25.2.5}$$

45
46
47
48
49
50
51
52
53
54
55
56
57
58
59
60
61
62
63
64
65
66
67
68
69
70
71
72
73
74
75
76
77
78
79
80
81
82
83
84
85
86

1 where R is the excess rainrate computed from
 2 Eq.(25.2.1), Δx and Δy are the pixel dimen-
 3 sions, $Q(i, t)$ is the outgoing discharge from pixel
 4 i at time t , and the summation is over all of the
 5 neighbor pixels that have D8-flow into pixel i .

6 Once Eq.(25.2.5) has been used to update V
 7 for each pixel, the grid of flow depths, d , can be
 8 updated using the channel geometry grids that
 9 give the length, bed width and bank angle of
 10 each channel. In the case of the kinematic wave
 11 approximation, the grids d and S can then be
 12 used to update the grid of flow velocities, u , using
 13 either Eq.(25.2.3) or Eq.(25.2.4). For an integral-
 14 equation version of the dynamic wave method,
 15 the velocity grid $\Delta u(i, t)$ would be incremented
 16 by an amount:

$$\begin{aligned}
 &= \left(\frac{\Delta t}{d(i, t) \cdot A_w} \right) \cdot \{u(i, t) \cdot Q(i, t) \cdot (C - 1) \\
 &+ \sum_{k \in N} [u(k, t) - u(i, t) \cdot C] \cdot Q(k, t) \\
 &- u(i, t) \cdot C \cdot R(i, t) \cdot \Delta x \cdot \Delta y \\
 &+ A_w \cdot [g \cdot d(i, t) \cdot S(i, t) - f(i, t) \cdot u^2(i, t)] \}
 \end{aligned} \tag{25.2.6}$$

17 where A_w is the wetted surface area of the bed,
 18 A_t is the top surface area of the channel and
 19 $C = A_w/A_t$. For overland grid cells, $C = 1$,
 20 and for channel grid cells $C > 1$. A_w and A_t
 21 are computed from the grid of channel lengths,
 22 L , and the assumed cross-sectional shape. In
 23 the last term, $f \equiv \tau_b/(\rho \cdot u^2)$ is a dimensionless
 24 friction factor:
 25

$$f = \left[\frac{\kappa}{\ln \left(a \cdot \frac{d}{z_0} \right)} \right]^2 \tag{25.2.7}$$

26 which corresponds to the law of the wall, while
 27 $f = g \cdot n^2 \cdot R_h^{-1/3}$ corresponds to Manning's
 28 equation. Instead of using the bed slope for S
 29 in Eq.(25.2.6), the water surface slope would be
 30 computed from the DEM, d and the D8 flow di-
 31 rection grid. As the numerical approach shown
 32 here is **explicit**, numerical stability requires a
 33 small enough time step such that water cannot
 34 flow across any grid cell in less than one time
 35 step. If u_m is the maximum velocity, then we
 36 require $\Delta t < \Delta x/u_m$ for stability.
 37

25.2.5 The overland flow process

38 The fundamental concept of **contributing area**
 39 was introduced in previous chapters (see §7).
 40 Grid cells with a sufficiently large contributing
 41 area will tend to have higher and more persist-
 42 ent surface fluxes and channelised flow. Con-
 43 versely, grid cells with small contributing areas
 44 will tend to have lower, intermittent fluxes. The
 45 intermittent nature of runoff-generating events,
 46 and the increased likelihood that small amounts
 47 of water will be fully consumed by infiltration or
 48 evapotranspiration make it even more likely that
 49 grid cells with small contributing areas will have
 50 little or no surface flux for much of the time. In
 51 addition, the **relative roughness** of the surface
 52 (typical height of roughness elements divided by
 53 the water depth) is higher for smaller contribut-
 54 ing areas so that frictional processes will be more
 55 efficient at slowing the flow. Under these circum-
 56 stances the shear stress¹ on the land-surface will
 57 tend to be too small to carve a channel or too
 58 infrequent to maintain a channel.
 59

60 Any surface flux will be as so-called **overland**
 61 or **Hortonian** flow and will tend to flow in a
 62 sheet that wets the entire bottom surface of a
 63 grid cell control volume during an event. This
 64 flow may be modelled with either a 1D or 2D
 65 approach, where the latter method would be re-
 66 quired to model flood events that exceed the
 67 bankfull channel depth, e.g. a dam break. In this
 68 case both channelised and overland flow must be
 69 modelled for channel grid cells.

70 Some models, such as CASC2D (Julien and
 71 Saghaian, 1991) have a **retention depth** (sur-
 72 face storage) that must be exceeded before over-
 73 land flow begins. Note that for sheet flow, the
 74 hydraulic radius, R_h is very closely approxi-
 75 mated by the flow depth, d . If w is the width
 76 of the grid cell projected in the direction of the
 77 flow, then the wetted area is given by $w d$ and
 78 the "*wetted perimeter*" is given by w . It follows
 79 that the hydraulic radius is equal to d . It has
 80 been found by Eagleson (1970) and many others
 81 since that Manning-type equations can be used
 82 to compute the flow velocity for overland flow,

¹Proportional to the square of the flow velocity.

1 but that a very large “Manning’s n ” value of
2 around 0.3 or higher is required, versus a typical
3 value of 0.03 for natural channels.

4 **25.2.6 The evaporation process**

5 Evaporation is a complex, essentially vertical
6 process that moves water from the Earth’s sur-
7 face and subsurface to the atmosphere. As with
8 the snowmelt process, the most sophisticated ap-
9 proach is based on a full surface energy balance
10 in which topographic effects can be incorporated
11 by including grids of slope and aspect in the solar
12 radiation model. However, since much of the re-
13 quired input data is typically unavailable, a num-
14 ber of simpler models have been proposed. The
15 **Priestley-Taylor** (Priestley and Taylor, 1972;
16 Rouse and Stewart, 1972; Rouse et al., 1977;
17 Zhang et al., 2000) and **Penman-Monteith**
18 models (Beven, 2000; Dingman, 2002) and their
19 variants are two simplified approaches that are
20 used widely. Sumner and Jacobs (2005) provide
21 a comparison of these and other methods.

22 Whatever method is used, the end result is
23 a grid sequence of evapotranspiration rates, E ,
24 that is then used in Eq.(25.2.1). Some dis-
25 tributed hydrologic models have additional rou-
26 tines for modelling the amount of water that is
27 moved from the root zone of the subsurface to
28 the atmosphere by the transpiration of plants.
29 A separate submodel is sometimes used to model
30 the variation of soil temperature with depth, es-
31 pecially for high-latitude applications.

32 **25.2.7 The infiltration process**

33 The process of infiltration is also primarily verti-
34 cal, but is arguably the most complex hydrologic
35 process at work in a basin. It has a first-order
36 effect on the hydrologic response of watersheds,
37 and is central to problems involving surface soil
38 moisture. It operates in the **unsaturated zone**
39 between the surface and the water table and rep-
40 represents an interplay between absorption due to
41 capillary action and the force of gravity. A vari-
42 ety of factors make realistic modelling of infiltra-
43 tion difficult, including the nature of boundary

conditions at the surface, between soil layers and 44
at the water table (a moving boundary). Vari- 45
ables such as hydraulic conductivity can vary 46
over orders of magnitude in both space and time 47
and the equations are strongly nonlinear. 48

As pointed out by many authors, including 49
Smith (2002), it is generally not sufficient to sim- 50
ply use spatial averages for input parameters, 51
and best methods for parameter estimation are 52
an active area of research. So-called macropores 53
may be present and must then be modelled sepa- 54
rately since they do not conform to the standard 55
notion of a porous medium. Discontinuous per- 56
mafrost may also be present in high-latitude wa- 57
tersheds. Smith (2002) provides an excellent re- 58
ference for infiltration theory, ranging from very 59
simple to advanced approaches. 60

Most spatial hydrologic models use a variant of 61
the **Green-Ampt** or **Smith-Parlange** method 62
for modelling infiltration (Smith, 2002). How- 63
ever, these are simplified approaches that are in- 64
tended for the relatively simple case where there 65
is: 66

- a single storm event, 67
- a single soil layer and 68
- no water table 69

While they can be useful for predicting flood 70
runoff, they are not able to address many other 71
problems of contemporary interest, such as: 72

1. redistribution of the soil moisture profile be- 73
tween runoff-producing events, 74
2. drying of surface layers due to evaporation 75
at the surface, 76
3. rainfall rates less than K_s (saturated hy- 77
draulic conductivity), 78
4. multiple soil layers with different properties, 79
and 80
5. the presence of a dynamic water table. 81

In order to address these issues and to model sur- 82
face soil moisture a more sophisticated approach 83
is required. 84

Infiltration in a porous medium is modelled with four basic quantities which vary spatially throughout the subsurface and with time. The **water content** (θ) is the fraction of a given volume of the porous medium that is occupied by water, and must therefore always be less than the **porosity**, ϕ . In the case of soils, θ represents the **soil moisture**. The **pressure head** (or capillary potential), ψ , is negative in the unsaturated zone and measures the strength of the capillary action. It is zero at the water table and positive below it. The **hydraulic conductivity**, K , has units of velocity and depends on the gravitational constant, the density and viscosity of water and the intrinsic permeability of the porous medium.

Darcy's Law, which serves as a good approximation for both saturated and unsaturated flow, implies that the vertical flow rate, v , is given by:

$$v = -K \cdot \frac{dH}{dz} = K \cdot \left(1 - \frac{d\psi}{dz}\right) \quad (25.2.8)$$

since $H = \psi - z$ (and z is positive downward). Conservation of mass for this problem takes the form:

$$\frac{\partial \theta}{\partial t} + \frac{\partial v}{\partial z} = J \quad (25.2.9)$$

where J is an optional source/sink term that can be used to model water extracted by plants. Inserting Eq.(25.2.8) into Eq.(25.2.9) we obtain **Richards' equation**:

$$\frac{\partial \theta}{\partial t} = \frac{\partial}{\partial z} \left[K \cdot \left(\frac{\partial \psi}{\partial z} - 1 \right) \right] \quad (25.2.10)$$

for vertical, one-dimensional unsaturated flow. Many spatial models solve this equation numerically to obtain a profile of soil moisture vs. depth for every grid cell, between the surface and a dynamic water table. However, in order to solve for the four variables, θ , ψ , K and v , two additional equations are required in addition to

Eq.(25.2.8) and Eq.(25.2.9). These extra equations have been determined empirically by extensive data analysis and are called **soil characteristic functions**.

The soil characteristic functions most often used are those of Brooks and Corey (1964), van Genuchten (1980) and Smith (1990). Each expresses K and ψ as functions of θ and contains parameters that depend on the porous medium under consideration (e.g. sand, silt, or loam).

The **transitional Brooks-Corey method** combines key advantages of the Brooks-Corey and van Genuchten methods (Smith, 1990), (Smith, 2002, pp.18-23). Water content, θ , is first rescaled to define a quantity called the **effective saturation**:

$$\Theta_e = \frac{\theta - \theta_r}{\theta_s - \theta_r} \quad (25.2.11)$$

that lies between zero and one. Here, θ_s is the **saturated water content** (slightly less than the porosity, ϕ) and θ_r is the **residual water content** (a lower limit that cannot be lowered via pressure gradients). Hydraulic conductivity is then modelled as:

$$K = K_s \cdot \Theta_e^\epsilon \quad (25.2.12)$$

where K_s is the **saturated hydraulic conductivity** (an upper bound on K) and $\epsilon = (2 + 3\lambda)/\lambda$, where λ is the **pore size distribution parameter**. Pressure head is modelled as:

$$\psi = \psi_B \cdot \left[\Theta_e^{-c/\lambda} - 1 \right]^{1/c} - \psi_a \quad (25.2.13)$$

where ψ_B is the **bubbling pressure** (or **air-entry tension**), ψ_a is a small shift parameter (which may be used to approximate hysteresis or set to zero), c is the **curvature parameter** which determines the shape of the curve near saturation.

1 Eqs.(25.2.8), (25.2.9), (25.2.12) and (25.2.13)
 2 provide a very flexible basic framework for mod-
 3 elling 1D infiltration in spatial hydrologic mod-
 4 els. The precipitation rate, P , the snowmelt
 5 rate, M , and evapotranspiration rate, E , are
 6 needed for the upper boundary condition. The
 7 vertical flow rate computed at the surface, v_0 ,
 8 determines I in Eq.(25.2.1).

9 **25.2.8 The subsurface flow process**

10 Once infiltrating water reaches the water table,
 11 the hydraulic gradient is such that it typically
 12 begins to move horizontally, roughly parallel to
 13 the land surface. The water table height may
 14 rise or fall depending on whether the net flux
 15 is downward (infiltration) or upward (exfiltra-
 16 tion, due to evapotranspiration). Darcy’s law
 17 (Eq.(25.2.8) continues to hold but $K = K_s$,
 18 $\theta = \theta_s \approx \phi$ and $\psi=0$ at the water table, with
 19 hydrostatic conditions ($\psi >0$) below it. More
 20 details on the equations used to model saturated
 21 flow are given by Freeze and Cherry (1979).

22 For shallow subsurface flow, various simplify-
 23 ing assumptions are often applicable, such as
 24 (1) the subsurface flow direction is the same
 25 as the surface flow direction and (2) the poros-
 26 ity decreases with depth. Under these circum-
 27 stances the water table height can be modelled
 28 as a grid that changes in time, using a control
 29 volume below each DEM grid cell that extends
 30 from the water table down to an impermeable
 31 lower surface (e.g. bedrock layer). Infiltration
 32 then adds water just above the water table at
 33 a rate determined from Richard’s equation and
 34 water moves laterally through the vertical faces
 35 at a rate determined by Darcy’s law. The dy-
 36 namic position of the water table is compared
 37 to the DEM; if it reaches the surface anywhere,
 38 then the rate at which water seeps to the sur-
 39 face provides a grid sequence, G , that is used in
 40 equation (25.2.1). Multiple layers, each with dif-
 41 ferent hydraulic properties and spatially-variable
 42 thickness can be modelled, but this increases the
 43 computational cost.

**25.2.9 Flow diversions: sinks, sources
 and canals**

44 Flow diversions are present in many watersheds
 45 and may be modelled as another “process”.
 46 Man-made canals or tunnels are often used to di-
 47 vert flow from one location to another, and usu-
 48 ally cannot be resolved by DEMs. They are typi-
 49 cally used for irrigation or urban water supplies.
 50 Tunnels may even carry flow from one side of a
 51 drainage divide to the other. Given the flow rate
 52 at the upstream end and other information such
 53 as the length of the diversion, these structures
 54 can be incorporated into distributed models. Di-
 55 versions can be modelled by providing a mecha-
 56 nism (outside of the D8 framework) for transfer-
 57 ring water between two non-adjacent grid cells.
 58 Sources and sinks may be man-made or natural
 59 and simply inject or remove flow from a point
 60 location at some rate. If the rate is known, their
 61 effect can also be modelled. It is increasingly un-
 62 common to find watersheds that are not subject
 63 to human influences.
 64
 65

**25.3 Scale issues in spatial
 hydrologic models**

66 While the preceding sections may give the im-
 67 pression that spatial hydrologic modelling is
 68 simply a straight-forward application of known
 69 physical laws, this is far from true. Many authors
 70 have pointed out that physically-based mathe-
 71 matical models developed and tested at a par-
 72 ticular scale (e.g. laboratory or plot) may be in-
 73 appropriate or at least gross simplifications when
 74 applied at much larger scales. In addition, het-
 75 erogeneity in natural systems (e.g. rainfall, snow-
 76 pack, vegetation, soil properties) means that
 77 some physical parameters appearing in models
 78 may vary considerably over distances that are
 79 well below the proposed model scale (grid spac-
 80 ing). It is therefore a nontrivial question as to
 81 how (or whether) a small number of “*point*” mea-
 82 surements can be used to set the parameters of
 83 a distributed model. **Variogram analysis** pro-
 84 vides one tool for addressing this problem and
 85 seeking a correlation length that may help to se-
 86
 87

lect an appropriate model scale. For some model parameters, remote sensing can provide an alternative to using point measurements.

The issue of **upscaling**, or how best to move between the measurement scale, process scale and model scale is very important and presents a major research challenge. A standard approach to this problem that has met with some success is the use of **effective parameters**. The idea is that using a representative value, such as a spatial average, might make it possible to apply a plot-scale mathematical model at the much larger scale of a model grid cell. Unfortunately, the models are usually nonlinear functions of their parameters so a simple spatial average is almost never appropriate. It is well-known in statistics that if X is some model parameter that varies spatially, f is a nonlinear² function and $Y = f(X)$ is a computed quantity, then $E[f(X)] \neq f(E[X])$. Here E is the expected value, akin to the spatial average. So, for example, the mean infiltration rate over a model grid cell (and associated net vertical flux) cannot be computed accurately by simply using mean soil properties (e.g. hydraulic conductivity) in Richards' equation.

An interesting variant of the effective parameter approach is to parameterize the subgrid variability of turbulent flow fields by replacing the molecular viscosity in the time-averaged model equations with an **eddy viscosity** that is allowed to vary spatially. This approach is successfully used by many ocean and climate models and may provide conceptual guidance for hydrologic modelers.

When it comes to the channel network and D8 flow between grid cells, upscaling is even more complicated because there is a fairly abrupt change in process dominance at the **hillslope scale** which marks the transition from overland to channelised flow. As seen in §7.6, this scale depends on the region and is needed in the pruning step when extracting a river network from a DEM. If the grid spacing is small enough to resolve the local hillslope scale, then it is possible to classify each grid cell as either hillslope

or channel. Each channel grid cell will typically contain a single channel with a width that is less than the grid spacing, as well as some “*hillslope area*”. Momentum balance can be modelled as long as channel properties such as length and bed width are stored for each grid cell, and the vertical resolution of the DEM is sufficient to compute the bed slope. However, if the grid spacing is larger than the hillslope scale, then a single grid cell may contain a dendritic network vs. a single channel. This is a much more complicated situation, but it may still be possible to get acceptable results by modelling flow in the cell's dendritic network with a single “*effective*” channel, using effective parameters.

Remark 120: *Physically-based mathematical models developed and tested at a particular scale (e.g. laboratory or plot) may be inappropriate or at least gross simplifications when applied at much larger scales. The issue of upscaling, or how best to move between the measurement scale, process scale and model scale is very important and represents a major research challenge.*

Using effective parameters and other upscaling methods, researchers have reported successful applications of spatial hydrologic models from the plot scale all the way up to the continental scale. Interestingly, the same model (e.g. MIKE SHE), but with very different parameter settings, can often be used at these two very different scales. While conventional wisdom suggests that traditional, lumped or semi-distributed models are better for large-scale applications, this has been largely for computational reasons and is becoming less of an issue. Note also that a distributed model is similar in many ways to a lumped model when a large grid spacing is used, although a lumped model may subdivide a watershed into a more natural set of linked control volumes.

Although much more work needs to be done on scaling issues, considerable guidance to mod-

²Anything other than $a \cdot X + b$.

1 elers is available in the literature. Examples of
 2 some good general references include Gupta et al.
 3 (1986); Blöschl and Sivapalan (1995); Blöschl
 4 (1999a) and Beven (2000). References for spe-
 5 cific processes include Dagan (1986) (ground-
 6 water), Gupta and Waymire (1993) (rainfall),
 7 Wood and Lakshmi (1993) (evaporation and en-
 8 ergy fluxes), Peckham (1995b) (channel network
 9 geometry and dynamics), Woolhiser et al. (1996)
 10 (overland flow), Blöschl (1999b) (snow hydro-
 11 logy) and Zhu and Mohanty (2004) (infiltration).

12 **25.4 Preprocessing tools for**
 13 **spatial hydrologic models**

14 As explained in the previous sections, most
 15 spatially-distributed hydrologic models make di-
 16 rect use of a DEM and several DEM-derived
 17 grids, including a flow direction grid (aspect),
 18 a slope grid and a contributing area grid. Ex-
 19 traction of these grids from a DEM with suffi-
 20 cient vertical and spatial resolution is therefore
 21 a necessary first step and may require depres-
 22 sion filling or burning in streamlines as already
 23 explained in detail in previous chapters (e.g. §4,
 24 §7). But spatially-distributed models require a
 25 fair amount of additional information to be spec-
 26 ified for every grid cell before any predictions can
 27 be made.

28 **Initial conditions** are one type of informa-
 29 tion that is required. Examples of initial con-
 30 ditions include the initial depth of water, the
 31 initial depth of snow, the initial water content
 32 (throughout the subsurface) and the initial posi-
 33 tion of the water table. Each of these examples
 34 represents the starting value of a dynamic vari-
 35 able that changes in time. **Channel geome-**
 36 **try** is another type of required information, but
 37 is given by static variables such as length, bed
 38 width, bed slope, bed roughness height and bank
 39 angle. Each of these must also be specified for
 40 every grid cell or corresponding channel segment.
 41 **Forcing variables** are yet another type of infor-
 42 mation that is required and they are often related
 43 to weather. Examples include the precipitation
 44 rate, air temperature, humidity, cloudiness, wind
 45 speed, and clear-sky solar radiation.

Each type of information discussed above can
 in principle be measured, but it is virtually im-
 possible to measure them for every grid cell in a
 watershed. As a result of this fact, these types
 of measurements are typically only available at a
 few locations (i.e. stations) as a time series, and
 interpolation methods (such as the inverse dis-
 tance method) must be used to estimate values
 at other locations and times. This important
 task is generally performed by a preprocessing
 tool, which may or may not be included with
 the distributed model.

Remark 121: *A variety of pre- and post-
 processing tools are required to support the
 use of spatial hydrologic models.*

Another important pre-processing step is to
 assign reasonable values for channel properties
 to every spatial grid cell. Some spatial hydro-
 logic models provide a preprocessing tool for this
 purpose. One method for doing this is to param-
 eterize them as best-fit, power-law functions of
 contributing area . That is, if A denotes a con-
 tributing area grid, then a grid of approximate
 channel widths can be computed via:

$$w = c \cdot (A + b)^p \tag{25.4.1}$$

where the parameters c , b and p are determined
 by a best fit to available data. The same ap-
 proach can be used to create grids of bed rough-
 ness values and bank angles. This approxima-
 tion is motivated by the well-known **empirical
 equations of hydraulic geometry** (Leopold
 et al., 1995) that express hydraulic variables as
 powers of discharge, and discharge as a power of
 contributing area. Measurements (e.g. channel
 widths) to determine best-fit parameters may be
 available at select locations such as gauging sta-
 tions, or may be estimated using high-resolution,
 remotely-sensed imagery.

For an initial condition such as flow depth,
 an iterative scheme (e.g. Newton-Raphson) can
 be used to find a steady-state solution given
 the channel geometry and a baseflow recharge

1 rate; this **normal flow** condition provides a rea-
 2 sonable initial condition. Alternately, a spatial
 3 model may be “*spun up*” from an initial state
 4 where flow depths are zero everywhere and run
 5 until a steady-state baseflow is achieved. Sim-
 6 ilar approaches could be used to estimate the
 7 initial position of the water table. Methods for
 8 estimating water table height based on wetness
 9 indices have also been proposed (see §7.6, §8.4.2
 10 and Beven (2000)). Any of these approaches may
 11 be implemented as a preprocessing tool.

12 When energy balance methods are used to
 13 model snowmelt or evapotranspiration, it is nec-
 14 essary to compute the net amount of shortwave
 15 and longwave radiation that is received by each
 16 grid cell. As part of this calculation one needs
 17 to compute the **clear-sky solar radiation** as a
 18 grid stack indexed by time. The concepts behind
 19 computing clear-sky radiation are discussed in
 20 §8.3.1 and are also reviewed by Dingman (2002,
 21 Appendix E). The calculation uses celestial me-
 22 chanics to compute the declination and zenith
 23 angle of the sun, as well as the times of local
 24 sunrise and sunset. It also takes the slope and as-
 25 pect of the terrain into account (as grids), along
 26 with several additional variables such as surface
 27 albedo, humidity, dustiness, cloudiness and opti-
 28 cal air mass. A general approach models direct,
 29 diffuse and backscattered radiation.

30 Another useful type of preprocessing tool is
 31 a rainfall simulator. One method for simulating
 32 space-time rainfall uses the mathematics of **mul-**
 33 **tifractal cascades** (Over and Gupta, 1996) and
 34 reproduces many of the space-time scaling prop-
 35 erties of convective rainfall.

36 It should be noted that DEMs with a vertical
 37 resolution of one meter do not permit a suffi-
 38 ciently accurate measurement of channel slope
 39 using the standard, local methods of geomor-
 40 phometry. Channel slopes are often between
 41 10^{-2} and 10^{-5} , but for a DEM with vertical and
 42 horizontal resolutions of 1 and 10 meters, respec-
 43 tively, the minimum resolvable (nonzero) slope is
 44 0.1. The author has developed an experimental
 45 “*profile-smoothing*” algorithm for addressing this
 46 issue that is available as a preprocessing tool in
 47 the TopoFlow model.

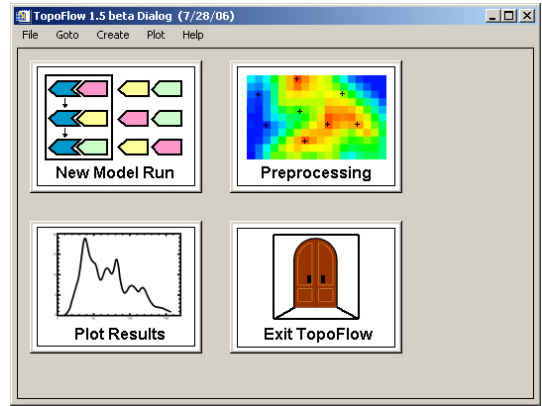


Fig. 25.3: The main panel in TopoFlow.

25.5 Case Study: hydrologic response of north basin, Baranja Hill

As a simple example of how a spatial hydrologic model can be used to simulate the hydrologic response of a watershed, in this section we will apply the TopoFlow model to a small watershed that drains to the northern edge of the Baranja Hill DEM. This is the largest complete watershed in the Baranja Hill DEM, an area in Eastern Croatia that is used for examples throughout this book.

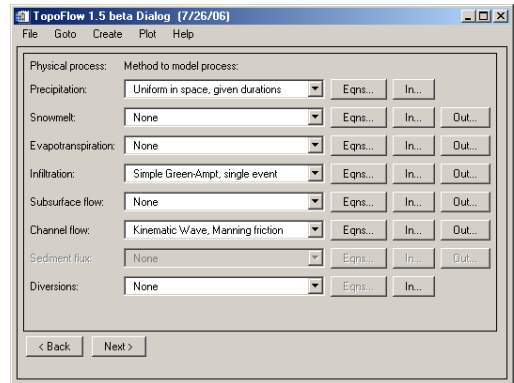
TopoFlow is a free, community-based, hydrologic model that has been developed by the author and colleagues. The TopoFlow project is an ongoing, open-source, collaborative effort between the author and a group of researchers at the University of Alaska, Fairbanks (L. Hinzman, M. Nolan and B. Bolton). This effort began with the idea of merging two spatial hydrologic models into one and adding a user-friendly, point-and-click interface. One of these models was a D8-based, rainfall-runoff model written by the author, which supported both kinematic and dynamic wave routing, as well as both Manning’s formula and the law of the wall for flow resistance. The second model, called ARHYTHM, was written by L. Hinzman and colleagues (Zhang et al., 2000) for the purpose of

1 modelling Arctic watersheds; it therefore contained
 2 advanced methods for modelling thermal processes such as snowmelt, evaporation and
 3 shallow-subsurface flow. In addition to its graphical user interface, TopoFlow now provides several
 4 different methods for modelling infiltration (from Green-Ampt to the 1D Richards' equation)
 5 and also has a rich set of preprocessing tools (Fig. 25.3). Examples of such tools include
 6 a rainfall simulator, a data interpolation tool, a channel property assignment tool and a clear-sky
 7 solar radiation calculator.

8 Before starting TopoFlow, RiverTools 3.0 (see §18) was used to clip a small DEM from the
 9 Baranja Hill DEM that contained just the north basin. This DEM had only 73 columns and 76
 10 rows, but the same grid spacing of 25 meters. It had minimum and maximum elevations of 85
 11 and 243 meters, respectively. RiverTools 3.0 was then used to extract several D8-based grids, including
 12 a flow direction grid, a slope grid, a flow distance grid and a contributing area grid. The
 13 drainage network above a selected outlet pixel (near the village of Popovac) was also extracted
 14 and had a contributing area of 1.84 square kilometers and a fairly large main-channel slope of
 15 0.04 [m/m]. RiverTools automatically performs pit-filling when necessary (see §7) but this was
 16 not much of an issue for this DEM because of its relatively steep slopes. Fig. 25.4 shows the D8
 17 flow lines for this small watershed, overlaid on a grid that shows the flow distance to the edge
 18 of the bounding rectangle with a rainbow colour scheme.

19 The TopoFlow model was then started as a plug-in from within RiverTools 3.0. It can
 20 also be started as a stand-alone application using the IDL Virtual Machine, a free tool that
 21 can be downloaded from ITT Visual Information Solutions (<http://www.itervis.com/idl/>).
 22 Fig. 25.5 shows the wizard panel in TopoFlow that is used to select which physical processes to
 23 model and which method to use for each process. Several methods are provided for modelling each
 24 hydrologic process, including both simple (e.g. degree-day, kinematic wave) and sophisticated
 25 (e.g. energy balance, dynamic wave) methods.

26 In this example, spatially uniform rainfall with a rate of 100 [mm/hr] and a duration of 4 minutes
 27 was selected for the Precipitation process, but gridded rainfall for a fixed duration or space-time
 28 rainfall as a grid stack of rainrates and a 1D array of durations could have been used. For the
 29 channel flow process, the kinematic wave method with Manning's formula for computing the flow
 30 velocity was selected. Clicking on the button labeled "In..." in the Channel Flow process row
 31 opened the dialog shown in Fig. 25.6.



32 Fig. 25.5: A dialog in the TopoFlow model that allows a user to select which method to use (if any) to model each hydrologic process from a droplist of choices. Once a choice has been selected, clicking on the "In..." or "Out..." buttons opens an additional dialog for entering the parameters required by that method. Clicking on the "Eqns..." button displays the set of equations that define the selected method.

33 All of the input dialogs in TopoFlow follow this same basic template; either a scalar value can be entered in the text box or the name of a file that contains a time series, grid or grid sequence. The filenames of the previously extracted D8-based grids for flow direction and slope (from RiverTools) were entered into the top two rows of this dialog. The filenames for Manning's *n*, channel bed width and channel bank angle as grids were entered in the next three rows. These were created with a preprocessing tool in TopoFlow's Create menu that uses a contributing area grid and power-law formulas to parameterize these quantities.

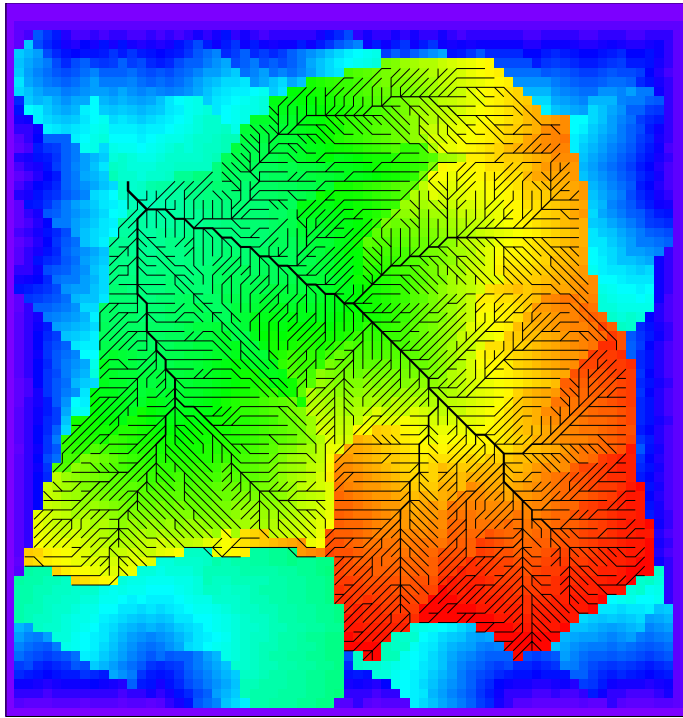


Fig. 25.4: Flow lines for the small basin near the north edge of the Baranja DEM, as extracted from a DEM by the D8 method. The flow lines are overlaid on a colour image that shows flow distance to the basin outlet.

1 If available, field measurements can be entered
 2 to automatically constrain the power-law param-
 3 eters, but for this case study default settings
 4 were used. This resulted in a largest channel
 5 width of 4.1 meters, which may be too large for
 6 such a small basin (1.84 km²). The correspond-
 7 ing value of Manning’s n was 0.02, which may
 8 similarly be too small. A value of 0.3 was used for
 9 overland flow. For this small watershed, a uni-
 10 form scalar value of 1.0 was used for the channel
 11 sinuosity. The initial flow depth was set to 0.0 for
 12 all pixels, although TopoFlow has another pre-
 13 processing tool for computing base-level channel
 14 flow depths in terms of an annual recharge rate
 15 and the other channel parameters. The channel
 16 process timestep at the bottom was set to a value
 17 of 3 seconds, as shown. This timestep was auto-
 18 matically estimated by TopoFlow as the largest
 19 timestep that would provide numerical stability.
 20 By clicking on the button labeled “Out...” in

the Channel Flow process row, the dialog shown
 in Fig. 25.7 was opened. This dialog allows a user
 to choose the type of output they want, and for
 which variables. TopoFlow allows user-selected
 output variables to be saved to files either as
 a time series (for one or more monitored grid
 cells) or as a grid stack indexed by time. The
 check boxes in Fig. 25.7 indicate that a grid stack
 and a time series (at the basin outlet) should be
 created for every output variable. A sampling
 timestep of one minute was selected; this gives
 a good resolution of the output curves (e.g. **hy-
 drograph**) but is much larger than the channel
 process timestep of 3 seconds that is required for
 numerical stability.

Once all of the input variables were set, the
 model was run with the infiltration process set
 to None. The resulting hydrograph is shown as
 the top curve in Fig. 25.10. The “*Simple Green-
 Ampt, single event*” method was then selected

21
22
23
24
25
26
27
28
29
30
31
32
33
34
35
36
37
38
39
40

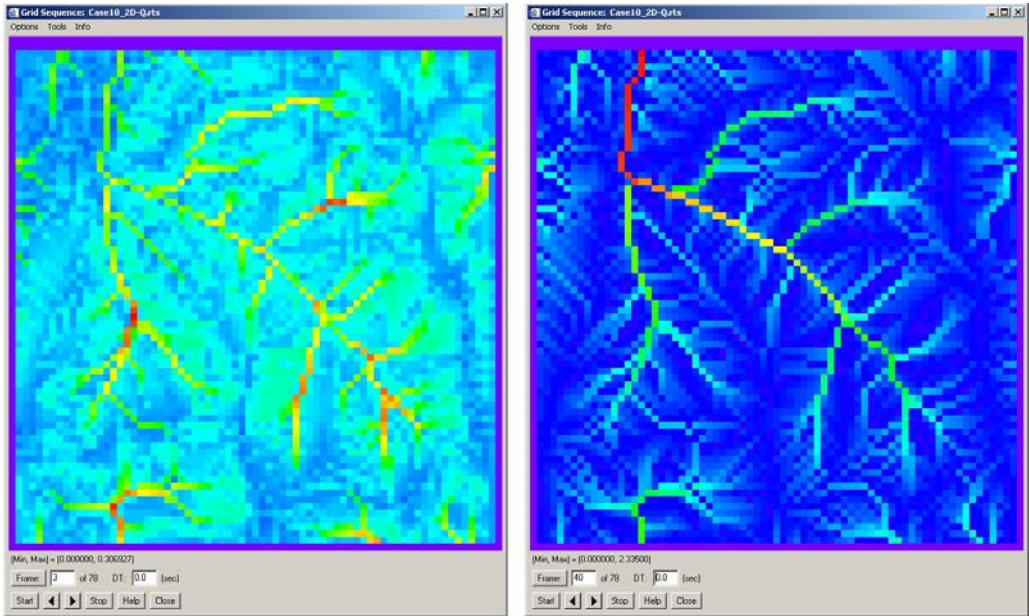


Fig. 25.9: The *Display* → *Grid Sequence* dialog in RiverTools 3.0 can be used to view grid stacks as animations or to view/query individual frames. The frame on the left is early in a simulation, and shows flood pulses starting to converge. The frame on the right shows the spatial pattern of discharge well into the storm.

1 from the droplist of available infiltration process
 2 methods. Clicking on the button labeled “In...”
 3 in the infiltration process row opened the dialog
 4 shown in Fig. 25.8. Toward the bottom of this
 5 dialog, “Clay loam” was selected as the closest
 6 standard soil type and the default input variables
 7 in the dialog were updated to ones typical of this
 8 soil type. The initial value of the soil moisture,
 9 shown as `theta_i` was changed from the default
 10 of 0.1 to the value 0.35. The infiltration process
 11 timestep listed toward the bottom of the dialog
 12 was changed to 3.0 seconds per timestep, in order
 13 to match³ the time-step of the channel flow pro-
 14 cess. When the model was run again with these
 15 settings, it produced the hydrograph shown as
 16 the bottom curve in Fig. 25.10. It can be seen
 17 that, as expected, the inclusion of infiltration
 18 resulted in a much smaller peak in the hydro-
 19 graph and also caused the peak to occur some-
 20 what later. At the end of a model run, any saved

³It can often be set to a much larger value (minutes to hours).

time series, such as a hydrograph, can be plotted
 with the *Plot* → *Function* option. Similarly, any
 grid stack can be visualized as a colour anima-
 tion with the *Plot* → *RTS File* option. The RTS
 (RiverTools Sequence) file format is a simple and
 efficient format for storing a grid stack of data.
 RTS files may be used to store input data, such
 as space-time rainfall, or output data, such as
 space-time discharge or water depth. RiverTools
 3.0 (see §18) has similar but more powerful visu-
 alization and query tools, including the *Display*
 → *Function* tool for functions (e.g. hydrographs
 and profiles), and the *Display* → *Grid Sequence*
 tool for grid stacks (see Fig. 25.9). The latter
 tool allows grid stacks to be viewed frame by
 frame or saved as AVI movie files. It also has
 several interactive tools such as (1) a Time Pro-
 file tool for instantly extracting a time series of
 values for any user-selected grid cell and (2) an
 Animated Profile tool for plotting the movement
 of flood waves along user-selected channels.

It is important to realise that TopoFlow can

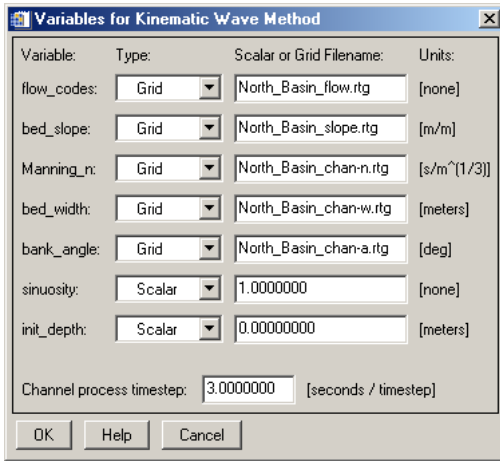


Fig. 25.6: The TopoFlow dialog used to enter required input variables for the “Kinematic Wave, Manning’s n” method of modelling channel flow. Notice that the data type (scalar, time series, grid or grid sequence) of each variable can be selected from a droplist. If the data type is “Grid”, then a filename is typed into the text box. These names refer to grids that were created with preprocessing tools. Units are always shown at the right edge of the dialog.

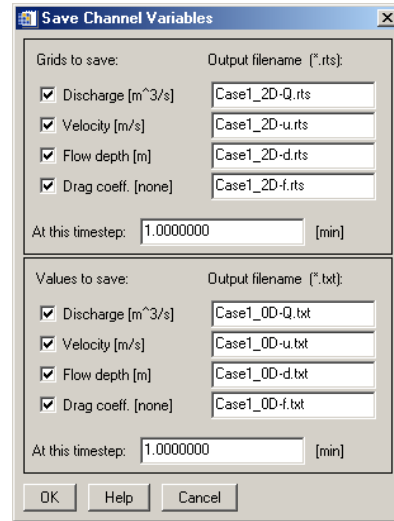


Fig. 25.7: The TopoFlow dialog used to choose how model output for the channel flow process is to be saved to files. Any output variable can be saved as either a time series for all monitored grid cells (in a multi-column text file) or as a sequence of grids. The time between saved values can be specified independently of the modelling timesteps.

1 perform much more complex simulations with-
 2 out much additional effort at run time. It allows
 3 virtually any input variable to any process to be
 4 entered as either a scalar (constant in space and
 5 time), a time series (constant in space, variable
 6 in time), a grid (variable in space, constant in
 7 time) or a grid stack (variable in space and time).
 8 It can also handle much larger grids than the one
 9 used in this case study. Advanced programming
 10 strategies including pointers, C-like structures,
 11 dynamic data typing and efficient I/O are used
 12 throughout TopoFlow for optimal performance
 13 and the ability to handle large data sets.

25.6 Summary points

15 Spatially-distributed hydrologic models make di-
 16 rect use of many geomorphometric variables.
 17 Flow direction or aspect is used to determine
 18 connectivity, or how water moves between neigh-
 19 bouring grid cells, and this same flow direction

is also commonly used for subsurface flow. Slope
 is one of the key variables needed to compute
 flow velocity for both overland and channelised
 flow. Both slope and aspect are used to compute
 clear-sky solar radiation, which may then be used
 by an energy-balance method to model rates
 of snowmelt and evapotranspiration. Channel
 lengths (between pixel centers) are used in com-
 puting flow resistance. Elevation can be used
 together with a lapse rate to estimate air tem-
 perature. Total contributing area can be used to
 determine whether overland or channelised flow
 is dominant in a given grid cell and can also be
 used together with scaling relationships to set
 channel geometry variables such as bed width
 and roughness for every grid cell.

One of the main advantages of spatially-
 distributed hydrologic models over other types
 of hydrological models is their ability to model
 the effects of human-induced change such as land
 use, dams, diversions, stream restoration, con-
 taminant transport, forest fires and global warm-

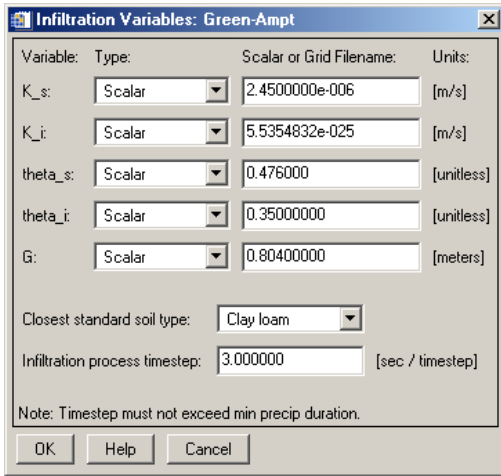


Fig. 25.8: The TopoFlow dialog used to enter required input variables for the “Green-Ampt, single event” method of modelling infiltration. Here, scalars have been entered for every variable and will be used for all grid cells. Choosing an entry from the “Closest standard soil type” droplist changes the input variable defaults accordingly and can be helpful for setting parameters when other information is lacking. This is also useful for educational purposes.

much work remains in order to resolve issues such as upscaling, these models can be extremely useful if applied with an understanding of their strengths and limitations. Clearly, results do depend on grid spacing, and the greatest uncertainties occur when grid cells are larger than the hillslope scale. For small to medium-sized basins, the problem of upscaling appears to be tractable and significant progress has already been made. Note that many of the problems such as sub-grid variability, modelling of momentum loss due to friction and specification of initial conditions are also encountered by fully-spatial climate and ocean models.

Remark 122: *Spatial hydrologic models can address many types of problems that cannot be addressed with simpler models, such as those that involve the effects of human-induced changes to all or part of a watershed.*

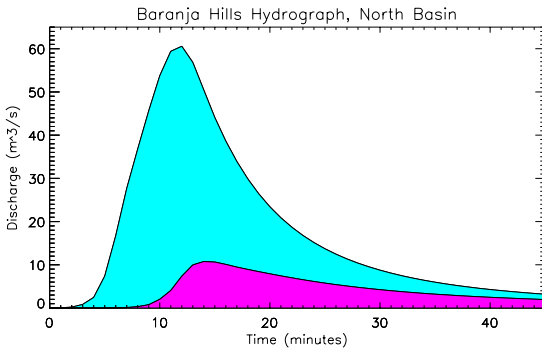


Fig. 25.10: Two hydrographs, showing how the hydrologic response of the small basin differs in two simple test cases. Both cases use spatially uniform rainrate, but one also includes the effect of infiltration via the Green-Ampt method.

In view of the large number of distributed models now used in hydrology and other fields, there is clearly a growing consensus that their advantages outweigh their disadvantages. A key attraction of physically-based, distributed models is that processes are modelled with parameters that have a physical meaning; note that even an effective parameter may have a well-defined physical meaning. These models also promote an integrated understanding of hydrology, rather than focusing on a particular process and neglecting others. These features combined with their visual appeal makes them very effective educational tools, especially when a variety of different methods are provided for modelling different processes, when any process can easily be turned off and when well-documented source code is made available.

Important sources:

- ★ Rivix LLC, 2004. RiverTools 3.0 User’s

1 ing. A truly amazing variety of problems can
 2 now be addressed with fully-spatial models that
 3 run on a standard personal computer. While

- 1 *Guide*. Rivix Limited Liability Company,
2 Broomfield, CO, 218 pp.
- 3 ★ Peckham, S.D., 2003. *Fluvial landscape*
4 *models and catchment-scale sediment trans-*
5 *port*. *Global and Planetary Change*, 39(1):
6 31-51.
- 7 ★ Blöschl, G., 2002. *Scale and Scaling in Hy-*
8 *drology — a Framework for Thinking and*
9 *Analysis*. John Wiley, Chichester, 352 pp.
- 10 ★ Beven, K.J., 2000. *Rainfall-Runoff Mod-*
11 *elling: The Primer*. John Wiley, New York,
12 360 pp.
- 13 ★ Beven, K.J., 1997. *TOPMODEL: A Cri-*
14 *tique*. *Hydrological Processes*, 11(9): 1069-
15 1086.